Advanced Materials Research Vols. 403-408 (2012) pp 4447-4455
Online available since 2011/Nov/29 at www.scientific.net
© (2012) Trans Tech Publications, Switzerland
doi:10.4028/www.scientific.net/AMR.403-408.4447

Error Modeling and Analysis of Inertial Measurement Unit using Stochastic and Deterministic Techniques

Zeeshan Ashraf[1] and Wajeeha Nafees[2]

[1]Faculty of Electronic Engineering, Ghulam Ishaq Khan Institute of Engineering Sciences & Technology, Topi, Khyber Pakhtunkhwa, Pakistan

[2]Dept. of Electrical Engineering, College of E&ME, National University of Sciences & Technology, Rawalpindi, Pakistan

email: zeeshan-ashraf@hotmail.com

email: engr.wajeeha@hotmail.com

Keywords-error modeling; IMU; deterministic; stochastic;

Abstract—The measurements provided by inertial measurement unit (IMU) are erroneous due to certain noise parameters which are needed to be taken into account because the corrupted data is of little practical value in inertial navigation systems (INS). By integrating the IMU data in navigation algorithm, these errors are accumulated, leading to significant drift in the attitude, position and velocity outputs. Several techniques have been devised for the error modeling of this error by way of Neural Networks (NNs), PSD, ARMA, etc. In this paper, the deterministic and stochastic approach is followed to model the noise parameters of a low cost IMU. The error parameters thus determined by using the both techniques help in the development of an effective navigation algorithm. Deterministic errors are calculated by the help of Up-Down Test and the Rate Table test. While the stochastic errors, which are more random in nature, are recognized using Power Spectral Density (PSD) Analysis and Allan Variance techniques.

Introduction

In the air-borne remote sensing environment, it is imperative to have correct measurements from the sensors. Although the low cost inertial measurement unit (IMU) have been utilized for navigation purposes, it is significantly important to characterize the noise parameters of these sensors. A standalone IMU is seldom used by itself since the inertial-sensor biases and fixed-step integration errors cause the navigation solution to diverge quickly. The flight path is determined by the navigation algorithm of the integrated navigation system which in this case was based on an inertial navigation system (INS) and a GPS receiver [1]. The algorithm counts on the measurements of INS. Any erroneous input from INS can result in the wrong flight path. Sensor parameters available in the datasheets always differ from the actual values. These parameters are subject to change because of temperature and fabrication variations. Sufficiently accurate modelling and understanding of the sensors and actuators is necessary to arrive at numerically efficient state estimation and control algorithms.

Several time-domain methods have been devised for stochastic modeling of the sensors. In [6], the Allan Variance method is described for the error modeling of inertial sensors. Some researchers also used the idea of Support Vector Machines for the error modeling of IMU [8]. Neural Networks are also been used for error modeling of gyros in [7] and [9]. This paper uses the deterministic as well as frequency-domain approach for modeling of noise parameters. Different methodologies have been followed for deterministic modeling while at the same time frequency-domain modeling is done for stochastic errors by using Power Spectral Density (PSD) and Allan variance method.

The IMU sensor that was used in this case was Sparkfun 6DOF Atomic IMU. It contained triple axis MMA7260Q accelerometer and three LISY300AL single axis gyros. The maximum measurable rate of gyros was 300 degrees per second. For error modeling of IMU, the deterministic errors include

Accelerometer Bias [5] or offset, Accelerometer scale factor error, Misalignment error, Gyro Drift or Bias and Gyro scale factor error [1], [2], [4]; the stochastic errors include Quantization error, White noise, Flicker noise and Random Walk [2].

The paper is organized in the following way. In Section II, the error analysis of IMU is done by elaborating all the techniques which were used to model the noise parameters and different data logging techniques using special arrangements with their results. The conclusion and the future recommendations are described in the last section that is Section III.

Error Modeling

Mathematical Model.

Accelerometers: the accelerometer error model can be expressed as:

$$\widetilde{a}_i = a_i + S_i a_i + B_i + n_i \tag{1}$$

where S_i is the scale factor, B_i is bias or offset and n_i is random noise in the signal [4]. To calculate bias of i^{th} axis, align that axis with earth's gravity vector so that accelerometer senses positive gravity a_1. Then rotate the sensor so that now the same i^{th} axis senses negative gravity a_2. Then bias and scale factor are given as,

$$B_i = \frac{a_1 + a_2}{2} \quad (\text{m/s}^2) \tag{2}$$

and

$$S_i = \frac{a_1 - a_2 - 2g}{2g} \quad (\text{unitless}) \tag{3}$$

respectively, where g is acceleration due to gravity.

Gyroscopes: The accelerometer error model can be expressed as:

$$\hat{w}_j = B_j + w_j + S_j w_j \tag{4}$$

where B_j is bias and S_j is scale factor. To calculate bias, rotate gyroscope at constant speed in clockwise direction and note w_1. Then rotate in counter-clockwise direction at same constant speed and note w_2. Bias and scale factor [2] are given as:

$$B_j = \frac{w_1 + w_2}{2} \quad (\text{rad/s}) \tag{5}$$

and

$$S_j = \frac{(w_1 - w_1 - 2w_e \sin\phi)}{2w_e \sin\phi} \quad (\text{unitless}) \tag{6}$$

respectively, where w_e is Earth's rotation speed and ϕ is the latitude of the gyroscope location.

Deterministic Errors.

Accelerometers: The accelerometer is calibrated using the "Up-Down test" in which earth's gravity is used as a reference to calibrate the accelerometers. The IMU is placed on a perfectly horizontal surface such that at one time only one of its axes is aligned with the earth's gravity component. The IMU is initially positioned so that its Z-axis is aligned with the local frame Up, U-axis, the Y-axis aligned with the North, N-axis and the X-axis aligned with the East, E-axis. This allows the gravity component to affect only the Z-axis of the accelerometer in the IMU. If the IMU is then rotated about the Y-axis, the accelerometer along the Z-axis senses negative gravity.

The data was collected for each of the three accelerometers X, Y and Z for a period of 30 minutes. After 30 minutes the IMU was rotated 180^o so that the effect of negative gravity could also be seen. In the static condition the vertical axis of the IMU faces an acceleration of 1g in one direction and -1g in the other. These readings were averaged out to obtain a mean value. Mathematical manipulations upon this mean gives a Bias value which is much closer to reality. The calibration for scale factor is done using a simple formula that gives a unit-less quantity. Fig. 1 shows the accelerometer output in g's which was obtained during the course of the up-down test.

The bias values obtained for all the three axes are enlisted in following table.

TABLE I. ACCELEROMETER BIAS

Accelerometer	Bias(m/s^2)
X axis	-0.579
Y axis	-0.7369
Z axis	-0.2105

Gyroscopes: The data of gyroscopes was logged on a test bench that was developed for slow rotation of our sensors [3] as shown in Fig. 2 and Fig. 3. A DC Encoder motor was utilized and feedback from the encoder was used to calculate the exact speed of the motor. Motor resolution was

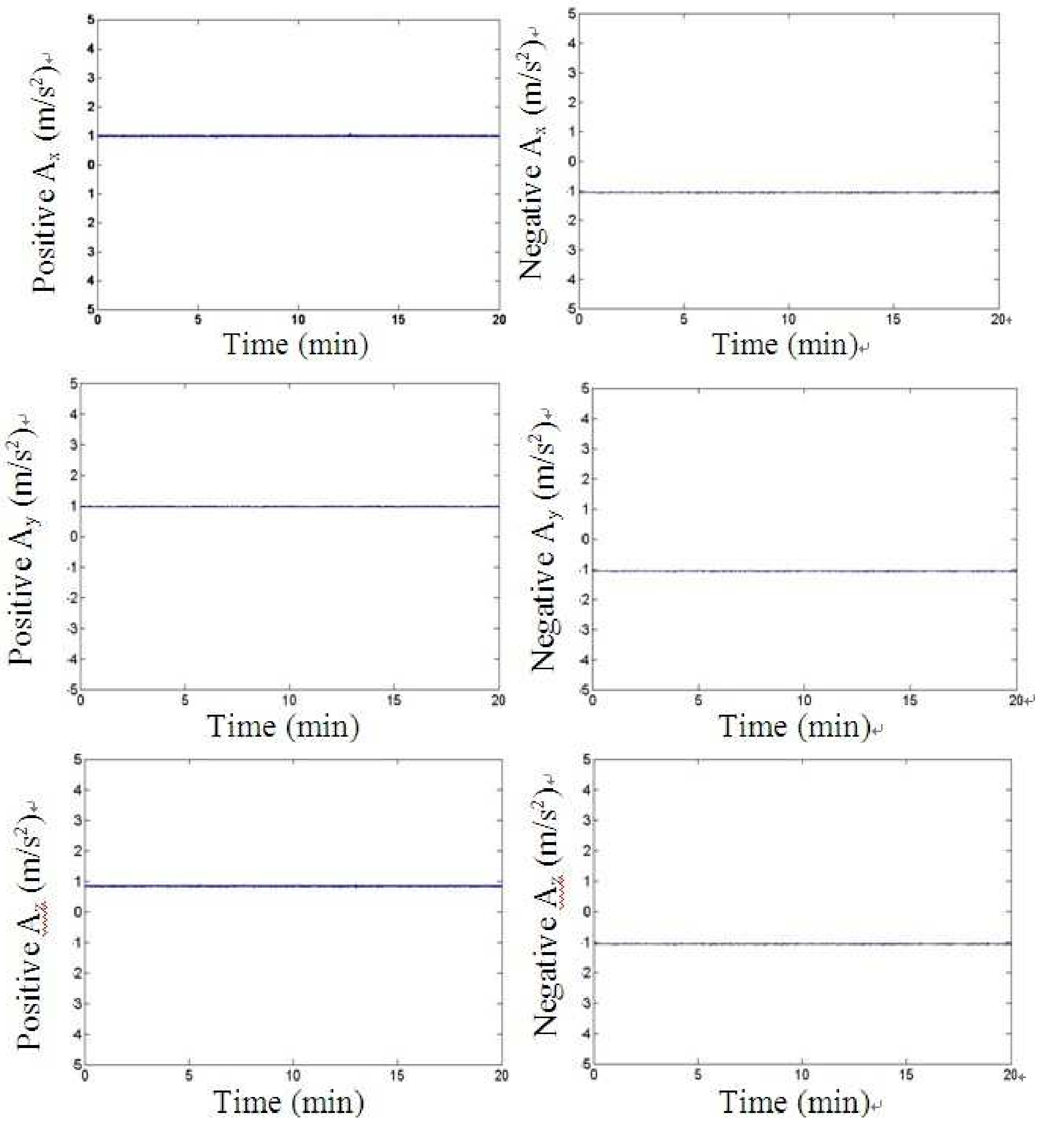

1024 slits per disc. An acrylic sheet was used to make a table like structure which was attached to the shaft of the motor as shown in Fig. 2. The sensors were fixed in the exact centre of the rate table so that the line of shaft passed exactly through the centre of gravity of the IMU. In this way an additional torque, which could be induced due to mismatch between the line of shaft and the centre of gravity of IMU, was avoided. Fig.3 shows how the IMU was fastened onto the rate table with the help of mounting screws. For each axis of the gyroscope, the rate table was rotated at constant speed not exceeding 300 degrees per second. The constant speed was maintained using the microcontroller programming. The table was first rotated in the clockwise (CW) direction, then in the counter-clockwise (CCW) direction. To calculate the speed of the rate table, feedback from the encoder of the motor was made input to the DSPIC 6014A. The calculated speed was further processed and sent to MATLAB R2008a by using Universal Asynchronous Receiver Transmitter (UART) module of DSPIC.

Figure 2. The Rate Table

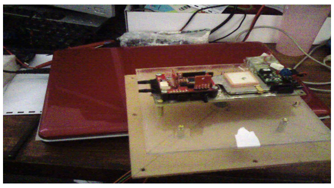

Figure 3. Gyroscope mounted on Rate Table

The output of gyroscopes was transmitted to MATLAB through an XBee Pro 900 transmitter, whose interface was already built-in in the IMU. The XBee Pro 900 Receiver interface was developed manually, using a single-layer printed circuit board (PCB). The output of gyros was also logged in MATLAB and a comparison was made between the calculated speed and measured speed from gyros in MATLAB.

Since the full scale reading of our gyro was ±300°/s, so the maximum speed that was measurable by the sensor was 0.833 Hz or 50 rpm. The motor was rotated at speeds less than the maximum. The following data was collected:

TABLE II. RATE TABLE TEST FOR ROLL AXIS

Table Speed (rev/min)	**Gyro Output (rpm) CW**	**Gyro Output (rpm) CCW**
10	10.5	10.3
20	19.8	20.1
25	25.4	22.5
30	31.1	30.7
35	35.1	35.6

TABLE III. RATE TABLE TEST FOR PITCH AXIS

Table Speed (rev/min)	**Gyro Output (rpm) CW**	**Gyro Output (rpm) CCW**
10	9.5	9.3
20	19.9	20.23
25	25.1	24.5
30	29.1	30.4
35	34.8	35.35

TABLE IV. RATE TABLE TEST FOR YAW AXIS

Table Speed (rev/min)	**Gyro Output (rpm) CW**	**Gyro Output (rpm) CCW**
10	10.4	10.25
20	19.85	20.2
25	25.9	23.7
30	30.1	30.9
35	33.9	35.25

The bias values for gyroscopes are listed below:

TABLE V. GYROSCOPE BIAS

Gyro	**Bias(^{0}/s)**
Roll	-6.83
Pitch	1.17
Yaw	-9.76

Stochastic Errors. The stochastic error in a measurement is the error that is random from one measurement to the next. Stochastic errors tend to be Gaussian, or *normal*, in their distribution. That's because the stochastic error is most often the sum of many random errors, and when we add many random errors together, the distribution of their sum looks Gaussian, as shown by the Central Limit Theorem. To estimate these errors, two techniques were conducted:

Power Spectral Density Method: Power spectral density is the amount of power per unit (density) of frequency (spectral) as a function of frequency. It describes how power or variance of a time series is distributed with frequency. It is also given as the Fourier transform of the autocorrelation sequence of a time series.

PSD graphs are in the form of log-log plots in which the horizontal axis has units of frequency and vertical has units of energy. The slopes of the graph depict what kinds of noise parameters are present in that sensor. One sided PSD estimate is given by (IEEE Std1293-1998):

$$S(f) = \frac{|X(f)|^2}{T} \tag{2}$$

where X(f) is fourier transform of the signal, T is product of sample time Δt and number of samples N. The PSD analysis plot obtained for y-accelerometer is shown in Fig. 4. The graph shows cluttering of data points at high frequency. It is difficult to extract out the parameters in this condition. So *Logarithmic Frequency Averaging Technique* [2] was applied to reduce the data points and simplify the identification of noise terms. In this technique the data points are averaged, so that in each of the N adjacent frequency level there is equal number of data points. This reduction of data points makes the PSD plots easier to comprehend. The results are plotted below:

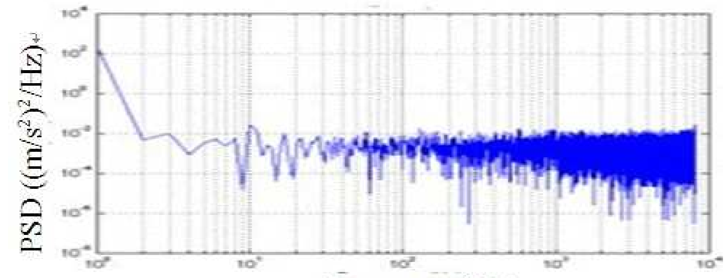

Figure 4. PSD Plot with Large number of Data points at High Frequencies

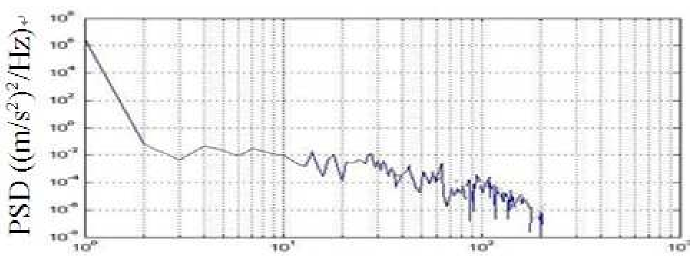

Figure 5. PSD Plot of Acc_x

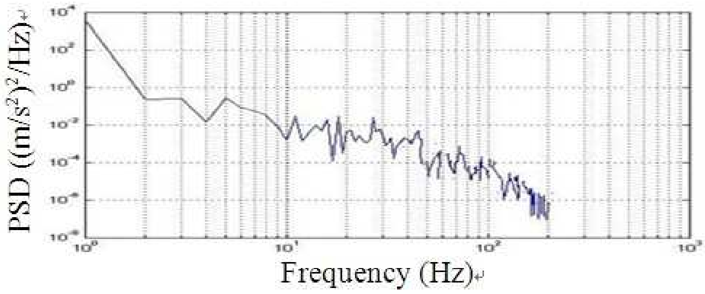

Figure 6. PSD Plot of Acc_y

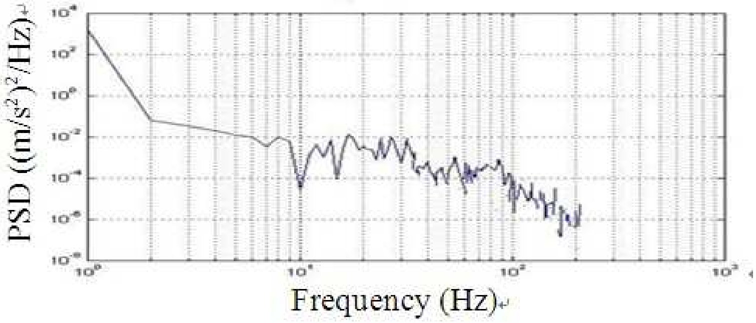

Figure 7. PSD Plot of Acc_z

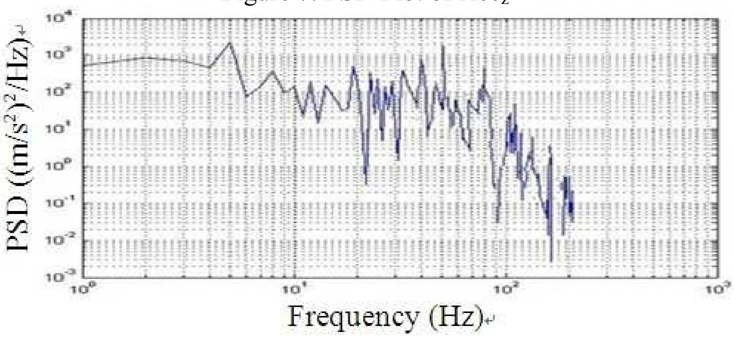

Figure 8. PSD Plot of Roll Rate

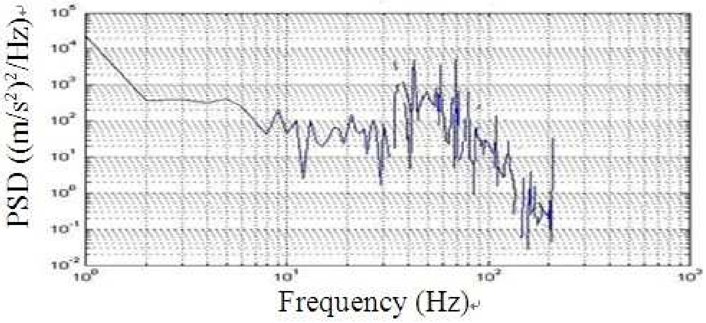

Figure 9. PSD Plot of Pitch Rate

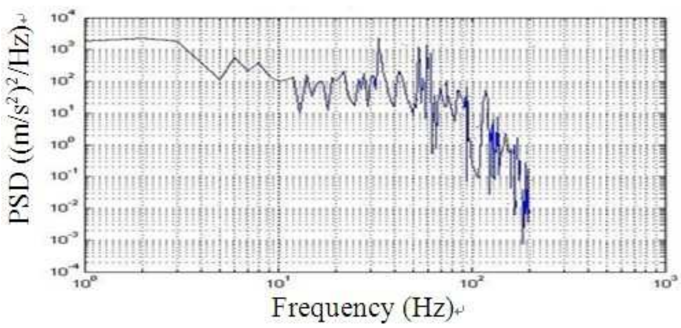

Figure 10. PSD Plot of Yaw Rate

Root Allan Variance Method: Allan variance is a time domain analysis technique. It is useful in determining the characteristics of the underlying random processes that give rise to the data noise. As such, it helps identify the source of a given noise term in the data. The Allan variance procedure executed here may be used as the only method of data analysis or to harmonize any of the frequency domain analysis techniques (PSD analysis). Slopes of Allan variance graph reveal the presence of several noise parameters in the sensor data.

The Allan variance of a given sequence is expressed as:

$$\sigma_a^2(\tau, N) \triangleq \frac{1}{2\left(\left[\frac{N}{n}\right]-1\right)} \sum_{j=0}^{\left[\frac{N}{n}\right]-2} \left[x_{j+1}(n) - x_j(n)\right]^2 . \tag{8}$$

In the following, an example is given to illustrate the principle.

Assume N=8. Then we calculate variance for n=1, 2, 4, 5, 6, 7, 8. Here the calculations for n=2 are discussed only.

n=2, $\tau = 2\Delta t$:

$$x_0(2) = \frac{y_0 + y_1}{2},\ x_1(2) = \frac{y_2 + y_3}{2} . \tag{9}$$

$$x_2(2) = \frac{y_4 + y_5}{2}, x_3(2) = \frac{y_6 + y_7}{2} \tag{10}$$

$$\sigma_a^2(2\Delta t, 8) = \frac{1}{2\cdot 3}\sum_{j=0}^{2}\left[x_{j+1}(2) - x_j(2)\right]^2 \tag{11}$$

$$\sigma_a^2(2\Delta t, 8) = \frac{1}{2\cdot 3}\sum_{j=0}^{2}\left[\frac{y_{2j+2} + y_{2j+3}}{2} - \frac{y_{2j} + y_{2j+1}}{2}\right]^2 . \tag{12}$$

The N data points are divided into clusters of n points [3]. In this paper, the value of N was taken to be 30000 and variable n was varied as 10, 50, 100, 500, 1000, 5000, 10000. The time step of the sensor was ΔT= 0.02s, resulting in averaging time τ (where τ= ΔT*n) of 0.2, 1, 2, 10, 20, 100, 200 seconds. Allan Variance was calculated [2] and results for all the six sensors are shown below:

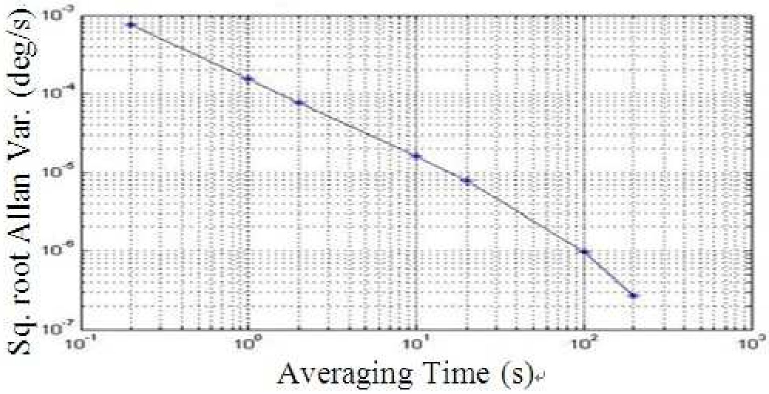

Figure 11. Root Allan Variance plot of Acc_x

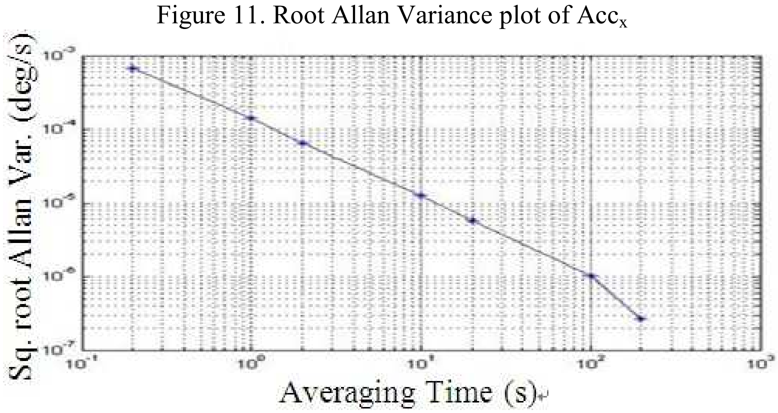

Figure 12. Root Allan Variance plot of Acc_y

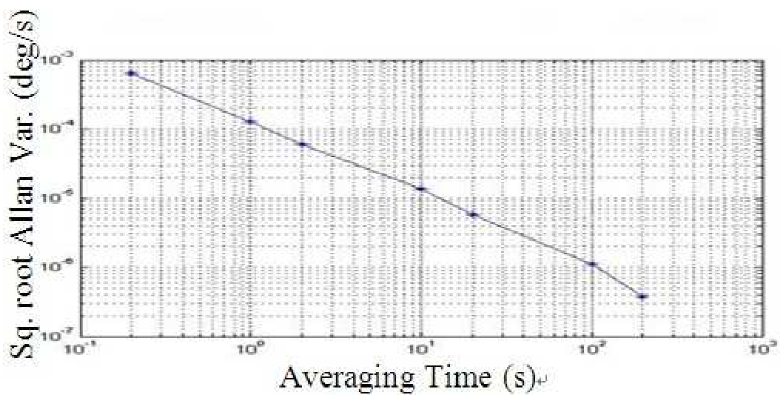

Figure 13. Root Allan Variance plot of Acc_z

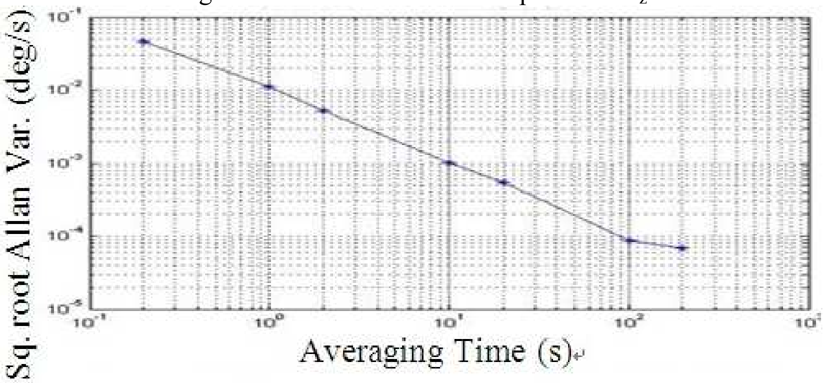

Figure 14. Root Allan Variance plot of Roll Rate

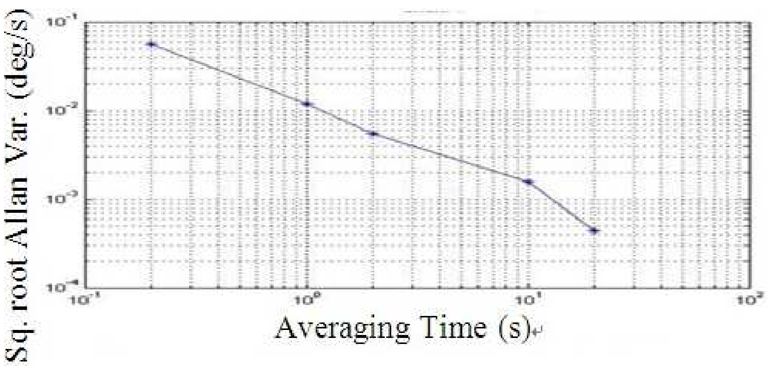

Figure 15. Root Allan Variance plot of Pitch Rate

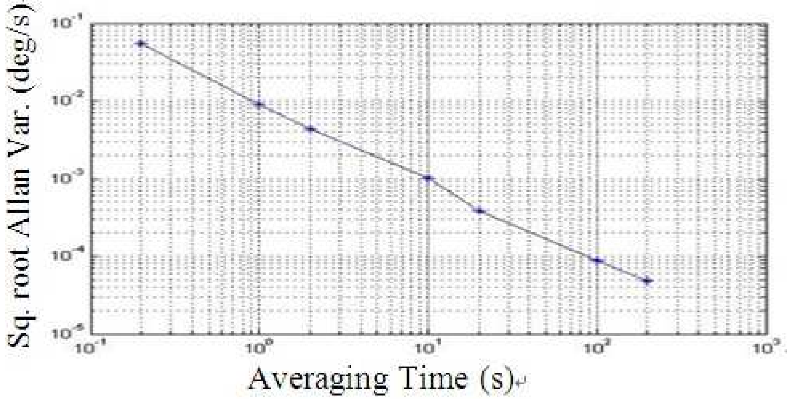

Figure 16. Root Allan Variance plot of Yaw Rate

The graphs of the aforementioned analytical methods were studied and noise parameters were calculated according to formulae given in [2], [3]. The following error terms were identified:

TABLE VI. GYROSCOPYE NOISE PARAMETERS

Noise Coefficient	Roll	Pitch	Yaw
Quantization Noise (rad)	0.0063	0.0051	0.0044
Angular White Noise (rad/√s)	1.2165e-4	9.798e-5	8.5991e-5
Angular Rate Flicker Noise (rad/s)	8.1877e-4	6.594e-4	5.7877e-4
Angular Rate Random Walk (rad/s/√s)	2.1070e-4	1.6791e-4	1.489e-4

TABLE VII. ACCELEROMETER NOISE PARAMETERS

Noise Coefficient	Acc x	Acc y	Acc z
Quantization Noise (m/s)	8.8462e-5	6.6658e-5	6.6159e-5
Velocity White Noise (m/s/√s)	1.7131e-6	1.2908e-6	1.2835e-6
Acceleration Flicker Noise (m/s^2)	1.153e-5	8.688e-6	8.623e-6
Acceleration Random Walk ($m/s^2/\sqrt{s}$)	2.9671e-6	2.2358e-6	2.2191e-6

Conclusion

The error modeling performed in this paper not only indicates the sort of errors present in the sensor, but also provides noise parameters of the sensors. These parameters are helpful in determining the error covariance matrix of the Kalman filter, used for state estimation through data fusion. The navigation filter implemented on the integrated navigation platform based on IMU and a GPS receiver can be validated by comparing the filter estimates with the corresponding calibrated errors. Initial tests performed on the rate table showed a need for a better and more robust rotation platform. When testing the IMU-sensors it is important to either monitor the ambient temperature or to stabilize the same temperature by temperature control or good insulation. The data logging can be improved by including a checksum check.

References

[1] Vikas Kumar N, “Integration of inertial navigation system and global positioning system using Kalman filtering,” M. Tech Dissertation, Indian Institute of Technology, Bombay. July 2004.

[2] Haiying Hou, “Modeling inertial sensor errors using Allan variance,” UCEGE reports number 20201. Master’s Thesis, University of Calgary, September 2004.

[3] Niklas Hjortsmarker, “Experimental system for validating GPS/INS integration algorithms,” Master’s Thesis, Lulea University of Technology, 2005

[4] Minha Park and Yang Gao, “Error analysis and stochastic modeling of low-cost MEMS accelerometer*”, J. Intell Robot Syst ,*vol. 46, no. 1, pp- 27-41.

[5] Senter Technology, “MEMS IMU Calibration Example”

[6] Naser El-Sheimy, Haiying Hou and Xiaoji Niu, “Analysis and Modeling of Inertial Sensors using Allan Variance”, IEEE Transactions on Instrumentation and Measurement, Vol. 57, no.1, January 2008.

[7] Wang Hao and Weifeng Tian, “Modeling the random drift of micro-machined gyroscope with neural network,” Neural Processing Letters, 2005, Vol. 22, no. 3, pp-235-247.

[8] Guoqiang Xu and Xiuyun Meng, “The MEMS IMU error modeling analysis using support vector machines,” Second International Symposium on Knowledge Acquisition and Modeling, 2009, pp-335-337.

[9] Chen Xiyuan, “Modeling random gyro drift by time series neural retwork and by traditional method,” Int. Conference on Neural Networks and Signal Processing, vol. 1, pp-810-813, 2003.

MEMS, NANO and Smart Systems

10.4028/www.scientific.net/AMR.403-408

Error Modeling and Analysis of Inertial Measurement Unit Using Stochastic and Deterministic Techniques

10.4028/www.scientific.net/AMR.403-408.4447